

International Telecommunication Union

**ITU-R**  
Radiocommunication Sector of ITU

**Recommendation ITU-R P.2146-0**  
(08/2022)

**Sea surface bistatic scattering**

**P Series**  
**Radiowave propagation**



## Foreword

The role of the Radiocommunication Sector is to ensure the rational, equitable, efficient and economical use of the radio-frequency spectrum by all radiocommunication services, including satellite services, and carry out studies without limit of frequency range on the basis of which Recommendations are adopted.

The regulatory and policy functions of the Radiocommunication Sector are performed by World and Regional Radiocommunication Conferences and Radiocommunication Assemblies supported by Study Groups.

## Policy on Intellectual Property Right (IPR)

ITU-R policy on IPR is described in the Common Patent Policy for ITU-T/ITU-R/ISO/IEC referenced in Resolution ITU-R 1. Forms to be used for the submission of patent statements and licensing declarations by patent holders are available from <http://www.itu.int/ITU-R/go/patents/en> where the Guidelines for Implementation of the Common Patent Policy for ITU-T/ITU-R/ISO/IEC and the ITU-R patent information database can also be found.

### Series of ITU-R Recommendations

(Also available online at <http://www.itu.int/publ/R-REC/en>)

Series	Title
<b>BO</b>	Satellite delivery
<b>BR</b>	Recording for production, archival and play-out; film for television
<b>BS</b>	Broadcasting service (sound)
<b>BT</b>	Broadcasting service (television)
<b>F</b>	Fixed service
<b>M</b>	Mobile, radiodetermination, amateur and related satellite services
<b>P</b>	<b>Radiowave propagation</b>
<b>RA</b>	Radio astronomy
<b>RS</b>	Remote sensing systems
<b>S</b>	Fixed-satellite service
<b>SA</b>	Space applications and meteorology
<b>SF</b>	Frequency sharing and coordination between fixed-satellite and fixed service systems
<b>SM</b>	Spectrum management
<b>SNG</b>	Satellite news gathering
<b>TF</b>	Time signals and frequency standards emissions
<b>V</b>	Vocabulary and related subjects

*Note: This ITU-R Recommendation was approved in English under the procedure detailed in Resolution ITU-R 1.*

Electronic Publication  
Geneva, 2022

© ITU 2022

All rights reserved. No part of this publication may be reproduced, by any means whatsoever, without written permission of ITU.

## RECOMMENDATION ITU-R P.2146-0

**Sea surface bistatic scattering**

(Question ITU-R 208-6/3)

(2022)

**Scope**

This Recommendation provides a method for predicting the bistatic scattering coefficient and coherent reflection coefficient for the sea surface. This model can be applied at any elevation angle, except grazing incidence, and is applicable for frequencies up to 100 GHz, and for wind speed between 0.5 m/s to 25 m/s.

**Keywords**

Bistatic scattering coefficient, coherent scattering, diffuse scattering, wind speed, upwind and crosswind mean square slopes, gravity wave, capillary wave, large-scale roughness, small-scale roughness

**Acronyms/Abbreviations**

ECMWF European Centre for Medium-Range Weather Forecast

ERA5 ECMWF Reanalysis version 5

**Related ITU-R Recommendations and Handbook**

Recommendation ITU-R P.372

Recommendation ITU-R P.452

Recommendation ITU-R P.527

Recommendation ITU-R P.528

Recommendation ITU-R P.676

Recommendation ITU-R P.680

Recommendation ITU-R P.1144

Recommendation ITU-R P.2148

NOTE – In every case, the latest revision/edition of the Recommendation in force should be used.

The ITU Radiocommunication Assembly,

*considering*

- a) that the proper planning of Earth surface observation systems and down-looking space systems, it is necessary to have appropriate models for predicting bistatic scattering coefficient of the sea surface;
- b) that the bistatic scattering coefficient may have one or two of the following components: coherent bistatic scattering coefficient component and diffuse (non-coherent) bistatic scattering coefficient component;
- c) that the diffuse bistatic scattering may be due to large-scale roughness driven by long gravity wave and small-scale roughness driven by short capillary wave;
- d) that both the long gravity wave and short capillary wave are driven by wind;

e) that model has been developed that allows the prediction of bistatic scattering coefficients of the sea surface needed in assessing several propagation parameters such as fading depth, atmospheric noise due to emission from sea surface, interference power due to scattering from sea surface,

*recommends*

that the method in the Annex should be used to predict the bistatic scattering coefficient from the sea surface.

## Annex

### TABLE OF CONTENTS

	<i>Page</i>
Policy on Intellectual Property Right (IPR).....	ii
Annex.....	2
1 Introduction .....	4
2 Step 0: Input parameters .....	6
2.1 Propagation input parameters .....	6
2.2 Sea surface input parameters .....	7
3 Step 1: Determine the sea the water complex relative permittivity.....	8
4 Step 2: Determine the sea surface roughness parameters.....	9
4.1 Sea surface small-scale height spectral density (capillary wave) and sea height variance.....	9
4.2 Probability density of large-scale probability density of surface slopes (gravity wave).....	9
5 Step 3: Determine the coherent bistatic scattering coefficient .....	10
6 Step 4: Determine the diffuse bistatic scattering due to large scale roughness.....	11
7 Step 5: Determine the diffuse bistatic scattering due to small-scale roughness.....	12
8 Sum the components of sea surface bistatic scattering coefficient .....	15
8.1 Sea surface backscattering coefficients .....	16
8.2 Sea surface bistatic scattering coefficients in the forward direction .....	18
Attachment A to Annex Calculation of scattering coefficients between circularly polarized and linearly polarized waves .....	22
A.1 Circularly Polarized (CP) incident to linear scattered power .....	22

A.2	Linear incident to CP scattered power.....	23
Attachment B to Annex	Calculation of scattering coefficients between circularly polarized waves .....	23
Attachment C to Annex	Simple approximations .....	24
Attachment D to Annex	Sea surface height spectra model.....	25
Attachment E to Annex	Interference power of a reflected signal from the sea surface into a receiver .....	26
E.1	Introduction.....	26
E.2	Coherent received power .....	27
E.3	Diffuse received power.....	28

## 1 Introduction

This Recommendation provides a method for predicting the sea surface bistatic scattering coefficient as a function of sea surface salinity, temperature, wind speed, relative wind direction and inverse wave age. If local data for these parameters are not available, the default values of these parameters as provided in Table 1 should be used. This prediction method is applicable to any elevation angle, except grazing incidence, any frequency up to 100 GHz, and wind speeds from 0.5 m/s to 25 m/s.

The bistatic scattering coefficient has two components: 1) a diffuse (non-coherent) component, which is the fraction of the incident power from an incident direction scattered to an arbitrary receive direction, and 2) a coherent component, which is the fraction of the incident power scattered back to the incident (i.e. specular) direction.

The prediction method in §§ 1 to 8 assumes the source and receiver polarizations are linear. If the source and/or receiver polarizations are circular, the appropriate bistatic scattering coefficients can be calculated from the linear bistatic scattering coefficients using the methods in Attachments A, B or C to this Annex.

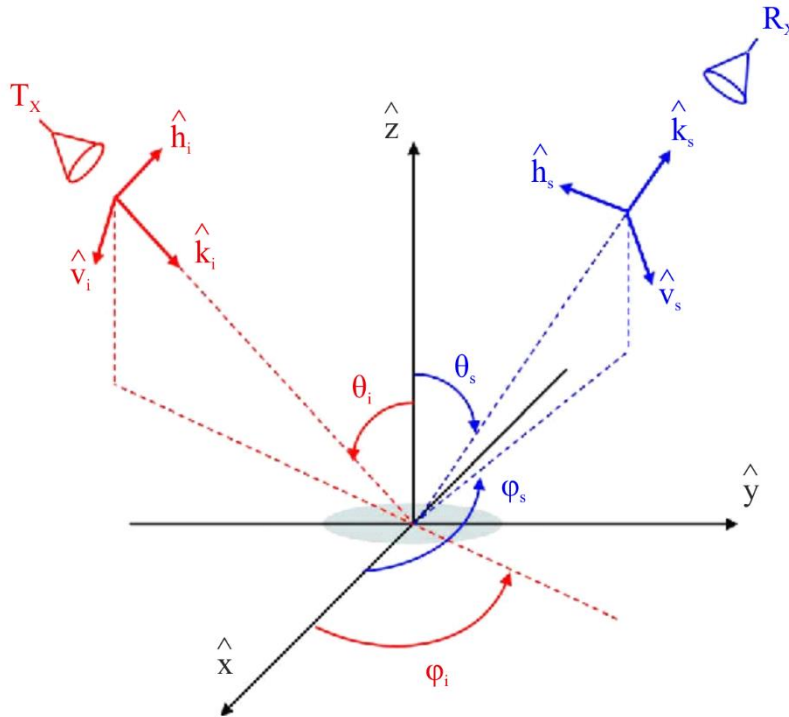
These prediction methods can be used to predict the interference power reflected by the sea surface between a source (e.g. a downlink transmitter) and a receiver receiving harmful interference (e.g. an Earth observation satellite receiver) using the method in Attachment E.

The sea surface is generally a randomly rough surface with roughness driven by wind. The bistatic scattering coefficient  $\gamma_{pq}(\hat{k}_s, \hat{k}_i)$  is the fraction of power scattered along a direction  $\hat{k}_s$  with polarization  $\hat{p}_s$  due to incident wave illuminating the surface along the direction  $\hat{k}_i$  with polarization  $\hat{q}_i$  (see Fig. 1). The fraction of power is per unit solid angle and per unit area. Due to the complex nature of the surface roughness, the bistatic scattering coefficient is assumed to be composed of two components: a coherent component  $\gamma_{pq}^c(\hat{k}_s, \hat{k}_i)$ , and a diffuse (non-coherent) component  $\gamma_{pq}^{dif}(\hat{k}_s, \hat{k}_i)$ . These two components are added together to:

$$\gamma_{pq}(\hat{k}_s, \hat{k}_i) = \gamma_{pq}^c(\hat{k}_s, \hat{k}_i) + \gamma_{pq}^{dif}(\hat{k}_s, \hat{k}_i) \quad (1)$$

The coherent component exists only along the specular direction of the surface ( $\theta_s = \theta_i$ ,  $\varphi_s = \varphi_i$ ).

FIGURE 1  
Geometric configuration of bistatic scattering from sea surface



P.2146-01

Figure 1 illustrates the geometry considered in the scattering model. The  $xy$ -plane is the horizontal sea surface and the zenith direction is the positive  $z$  axis. The positive  $x$  axis is the upwind<sup>1</sup> direction, the positive  $y$  axis is the crosswind direction where the incidence zenith angle,  $\theta_i$  and the scattering zenith angle,  $\theta_s$ , are measured from the positive  $z$  axis. The incidence clock angle,  $\varphi_i$ , and the scattering clock angle,  $\varphi_s$  are measured in the  $xy$ -plane in the counter-clockwise direction relative to the upwind direction.

The sea surface is treated as a two-scale roughness surface having large-scale roughness and small-scale roughness laying over the long-scale roughness. The long-scale roughness is associated with the long gravity wave and the small-scale roughness is associated with the short capillary wave. Accordingly, the diffuse (non-coherent) component of the bistatic scattering coefficient  $\gamma_{pq}^{dif}(\hat{k}_s, \hat{k}_i)$  is the sum of two components as given in equation (2):

$$\gamma_{pq}^{dif}(\hat{k}_s, \hat{k}_i) = \gamma_{pq}^l(\hat{k}_s, \hat{k}_i) + \gamma_{pq}^s(\hat{k}_s, \hat{k}_i) \quad (2)$$

The first term in equation (2) is attributed to the sea surface long-scale roughness and the second term is attributed to the small-scale roughness.

The model for predicting the coherent and the diffuse (non-coherent) components of the sea surface bistatic scattering coefficient can be constructed based on the flow chart depicted in Fig. 2.

<sup>1</sup> The upwind direction is the opposite direction that the wind is heading.

FIGURE 2

**Flow chart of the sea surface bistatic scattering prediction model****Step 0**Determine input parameters (section 2)**Step 1**Determine complex relative permittivity (section 3)**Step 2**Determine the surface roughness parameters (section 4)**Step 3**Determine coherent bistatic scattering coefficient (section 5)**Step 4**Determine diffuse bistatic scattering coefficient component due to large scale roughness (section 6)**Step 5**Determine diffuse bistatic scattering coefficient component due to short scale roughness (section 7)**Step 6**Sum the components of bistatic scattering coefficient (section 8)

P.2146-02

The bistatic scattering coefficient of sea surface modelled here is for linearly polarized incident waves and linearly polarized scattered waves. The transformations from a linear polarization basis to other combinations of incident and scattered polarizations are provided in Attachment A and Attachment B:

- Attachment A is for circularly polarized incident waves and linearly polarized scattered waves and vice versa.
- Attachment B is for circularly polarized incident waves and circularly polarized scattered waves.
- Attachment C provides simple approximations for the bistatic scattering coefficients in Attachment A and Attachment B.

Moreover,

- Attachment D provides a sea surface height spectra model.
- Attachment E provides a methodology for determining the interference power from a reflected/scattered signal of the sea surface into a receiver

## 2 Step 0: Input parameters

To predict values of the coherent and diffuse (non-coherent) components of the bistatic scattering coefficient for sea surface, two types of input parameters are required:

- Propagation input parameters, and
- Sea surface input parameters.

### 2.1 Propagation input parameters

The propagation input parameters are as follows:



- The elevation angle  $\epsilon_i$  and azimuth angle  $\varphi_i$  of the incident wave illuminating the sea surface. These two angles determine the incident propagation direction  $\hat{k}_i$ .
- The polarization vector  $\hat{q}_i$  of the wave illuminating the sea surface.
- The elevation angle  $\epsilon_s$  and azimuth angle  $\varphi_s$  of the scattering direction  $\hat{k}_s$  along which the bistatic scattering coefficient is calculated.
- The polarization vectors  $\hat{p}_s$  of the scattered field.
- The frequency  $f$  at which the bistatic scattering coefficient is calculated. The frequency is given in GHz units. The frequency determines the RF wavenumber  $k$  ( $k = 2\pi f / 0.299792458$  rad/m).

Since only linear polarizations are considered in this Annex,  $\hat{q}_i = \hat{v}_i$  or  $\hat{h}_i$  and  $\hat{p}_s = \hat{v}_s$  or  $\hat{h}_s$  with  $v$  standing for vertical (parallel) polarization, and  $h$  standing for horizontal (perpendicular) polarization. Throughout this recommendation the elevation angles  $\epsilon_{i,s}$  are replaced by the corresponding zenith angles  $\theta_{i,s}$ .

$$\theta_{i,s} = \frac{\pi}{2} - \epsilon_{i,s} \quad (3)$$

## 2.2 Sea surface input parameters

The sea surface input parameters required for predicting bistatic scattering from sea surface are reported in Table 1 where default values may be used if local parameters are not known.

TABLE 1  
Sea surface input parameters

Parameter	Description	Default value
Sea surface salinity	Required for computing the complex relative permittivity of sea surface	35 ppt <sup>2</sup>
Sea surface temperature	Required for computing the complex relative permittivity of sea surface	0, 15, 30° C
Wind speed $U_{10}$ (m/s)	The wind speed at a height of 10 m above sea surface	See text below
Inverse wave age $\Omega$	The sea is fully developed when $\Omega$ is close to 0.85, mature when $\Omega$ is close to 1, and young when $\Omega > 2$	0.85
Cut off roughness height wavenumber $\kappa_d$	The height wavenumber dividing the sea surface height spectrum into long gravity wave spectrum and short capillary wave spectrum	$0.5k$ where $k$ is the wavenumber (1/m)

### Wind speed and coordinate system

Local values of the parameters in Table 1 should be used if available. Wind speed at 10 m above the sea surface depends on geographic location and season and varies over time. If available, local sea surface wind speed data (magnitude, direction and spatial and temporal correlation) applicable to the

<sup>2</sup> The unit ppt is parts per thousand.

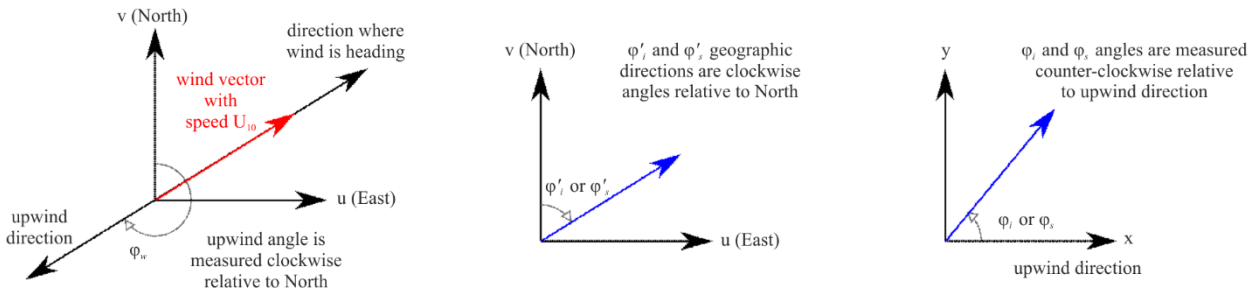
specific geographical location of interest should be used. If spatial or temporal correlation is not required, the global maps in Recommendation ITU-R P.2148 can be used.

If local sea surface wind speed data are not available, the local temporal wind vector can be derived from multiple sources of global data; e.g. the eastward and northward components of hourly wind speed at a height of 10 m above the surface of the Earth from 1979 are available from the ECMWF Copernicus Climate Data Store.

Some datasets (e.g. ECMWF ERA5 data) provide the  $v$ , northward (wind heading towards the north) component of wind speed, and the  $u$ , eastward (wind heading toward the east) component of wind speed. For a given value of  $u$  and  $v$ , the magnitude of the wind speed at a height of 10 m above the surface of the Earth,  $U_{10}$ , is  $\sqrt{u^2 + v^2}$ . As shown in Fig. 3, the upwind direction is the opposite direction that the wind is heading; and the clockwise angle from north to the upwind direction,  $\varphi_w$ , is  $270^\circ - \text{atan2}(v, u)$ <sup>3</sup>. Hence, in Fig. 3, the positive  $x$ -axis, which corresponds to the upwind direction, is a clockwise angle of  $270^\circ - \text{atan2}(v, u)$  relative to north; or, equivalently, north is a counter clockwise angle of  $270^\circ - \text{atan2}(v, u)$  relative to the upwind direction.

If  $\varphi'_i$  and  $\varphi'_s$  are the incident and scattering clockwise angles relative to north, then  $\varphi_i$  and  $\varphi_s$ , the corresponding incident and scattering clockwise angles shown in Fig. 3 are:  $\varphi_i = \varphi_w - \varphi'_i$  and  $\varphi_s = \varphi_w - \varphi'_s$ .

FIGURE 3  
Wind speed and coordinate systems



P.2146-03

The following intermediate parameters are calculated from the above input parameters as part of the method:

- Sea surface complex relative permittivity  $\epsilon_r$ ,
- Sea surface height spectral density function  $W_S(\kappa, \psi)$ ,
- Sea surface height variance  $\sigma^2$ , and
- Sea surface upwind and cross wind mean square slopes  $m_u^2$  and  $m_c^2$ .

### 3 Step 1: Determine the sea the water complex relative permittivity

The complex relative permittivity model described by equations (14) to (27) of Recommendation ITU-R P.527-6 is used in this Recommendation to obtain the sea water complex relative permittivity. This model formulates the sea water complex relative permittivity  $\epsilon_r$  in terms of sea surface salinity,

<sup>3</sup> The function  $\text{atan2}(y, x)$  is defined as the angle between the positive  $x$  axis and the vector from the origin to the point  $(x, y)$ .

sea surface temperature and RF frequency. The default values of sea surface salinity and temperature are given in Table 1.

#### 4 Step 2: Determine the sea surface roughness parameters

Sea surface roughness is described by the following:

- The small-scale surface height spectral density which is required for calculating the diffuse bistatic scattering coefficient component due to small-scale roughness (§ 6).
- The total sea surface rms height which is required for calculating the coherent reflectivity (§ 5).
- The large-scale probability density of surface slopes which is required for calculating the diffuse bistatic scattering coefficient component due to large scale roughness (§ 7).

##### 4.1 Sea surface small-scale height spectral density (capillary wave) and sea height variance

The small-scale spectrum is related to the sea surface directional spectrum,  $W(\kappa, \psi)$ , as follows.

$$W_s(\kappa, \psi) = \begin{cases} 0 & \text{if } \kappa < \kappa_d \\ W(\kappa, \psi) & \text{otherwise} \end{cases} \quad (4)$$

where  $\kappa_d$  is the two-scale cut-off height wavenumber, and  $(\kappa, \psi)$  are the polar coordinates of the spatial wavenumbers in the upwind and crosswind directions associated with the rectangular coordinates of the surface slopes. Explicit expression for  $W(\kappa, \psi)$  is given in Attachment D.

The total sea surface rms height  $\sigma$ , which is required for calculating the coherent reflectivity, is related to the wind speed,  $U_{10}$ , as follows:

$$\sigma^2 = \begin{cases} \sigma_0 + \sigma_1 U_{10} + \sigma_2 U_{10}^2 + \sigma_3 U_{10}^3 + \sigma_4 U_{10}^4 + \sigma_5 U_{10}^5 & \text{if } U_{10} \geq 1 \text{ m/s} \\ 0.001515 U_{10} & \text{if } U_{10} < 1 \text{ m/s} \end{cases} \quad (5)$$

With  $\sigma^2$  (the surface height variance) in square meters and  $U_{10}$  (wind speed at a height of 10 m above sea surface) in m/s, and:

$$\sigma_0 = -0.002913931483264$$

$$\sigma_1 = 0.006483314256661$$

$$\sigma_2 = -0.002390537892927$$

$$\sigma_3 = 0.000309146709141$$

$$\sigma_4 = 0.000026373965831$$

$$\sigma_5 = 0.000000350137099$$

##### 4.2 Probability density of large-scale probability density of surface slopes (gravity wave)

The large-scale probability density of surface slopes is represented by zero-mean bivariate Gaussian distribution:

$$P(S_u, S_c) = \frac{1}{2\pi m_u m_c} \exp \left\{ -\frac{1}{2} \left( \frac{S_u^2}{m_u^2} + \frac{S_c^2}{m_c^2} \right) \right\} \quad (6)$$

where  $S_u$  and  $S_c$  are the slopes along the upwind and crosswind directions at surface patches where local bistatic scattering coefficients are calculated. Furthermore,  $m_u^2$  and  $m_c^2$  are the upwind and crosswind mean square slopes.

$$m_u^2 = \sum_{t=0}^7 a_t U_{10}^t \quad (7)$$

$$m_c^2 = \sum_{t=0}^7 b_t U_{10}^t \quad (8)$$

where the regression coefficients  $a_t$  ( $t = 0, \dots, 7$ ) and  $b_t$  ( $t = 0, \dots, 7$ ) in equations (7) and (8) have the following dependence on frequency  $f$  in GHz:

$$a_t = d_{t,0} + d_{t,1} \log_e f + d_{t,2} (\log_e f)^2 + d_{t,3} (\log_e f)^3 + d_{t,4} (\log_e f)^4 \quad t = 0, \dots, 7 \quad (9)$$

$$b_t = z_{t,0} + z_{t,1} \log_e f + z_{t,2} (\log_e f)^2 + z_{t,3} (\log_e f)^3 + z_{t,4} (\log_e f)^4 \quad t = 0, \dots, 7 \quad (10)$$

The coefficients  $d_{t,m}$  and  $z_{t,m}$  are given in Table 2 and Table 3, respectively. Equations (7) and (8) are valid for  $U_{10}$  values between 0.5 m/s and 25 m/s and frequencies between 1 and 100 GHz.

TABLE 2

Values of the regression coefficients  $d_{t,m}$  of equation (9)

$a_t$	$d_{t,0}$	$d_{t,1}$	$d_{t,2}$	$d_{t,3}$	$d_{t,4}$
$a_0$	-0.001 316 803 829	-0.000 766 377 24	0.000 178 465 995	0.000 163 583 254	-2.722 372 719 5e-05
$a_1$	0.003 381 740 504	0.003 262 226 696	0.001 055 843 558	-0.000 556 018 050	5.638 297 081 0e-05
$a_2$	-8.387 091 908e-06	-0.000 788 099 04	-0.000 849 564 4	0.000 321 034 03	-2.969 409 304 3e-05
$a_3$	-7.172 344 345 1e-05	9.130 847 487e-05	0.000 180 310 43	-6.039 065 778e-05	5.252 298 53e-06
$a_4$	9.781 960 983 7e-06	-5.515 385 070e-06	-1.831 052 853e-05	5.756 933 90e-06	-4.820 426 74e-07
$a_5$	-5.824 151 735 3e-07	1.831 590 630e-07	9.693 536 66e-07	-2.928 018 73e-07	2.384 386 09e-08
$a_6$	1.662 701 734 3e-08	-3.121 665 19e-09	-2.590 444 81e-08	7.608 802 794e-09	-6.063 116 61e-10
$a_7$	-1.853 308 18e-10	2.084 451 182e-11	2.762 769 59e-10	-7.94818760e-11	6.223 677 47e-12

TABLE 3

Values of the regression coefficients  $z_{t,m}$  of equation (10)

$b_t$	$z_{t,0}$	$z_{t,1}$	$z_{t,2}$	$z_{t,3}$	$z_{t,4}$
$b_0$	-0.000 388 356 64	-0.000 566 882 739	-0.000 187 663 9	0.000 195 168 030 1	-2.564 879 98e-05
$b_1$	0.000 711 554 432 3	0.001 274 333 859	0.001 582 455 599	-0.000 564 251 194	5.158 545 58e-05
$b_2$	0.000 467 115 768	7.665 602 489e-05	-0.000 999 944 82	0.000 304 430 724	-2.608 628 437e-05
$b_3$	-0.000 113 274 18	-7.062 890 94e-05	0.000 204 604 176	-5.704 760 441e-05	4.619 116 82e-06
$b_4$	1.144 869 515e-05	9.917 914 997 6e-06	-2.031 787 86e-05	5.376 554 489e-06	-4.184 881 982e-07
$b_5$	-5.954 866 288 2e-07	-6.127 030 44e-07	1.063 995 76e-06	-2.717 537 12e-07	2.052 809 6e-08
$b_6$	1.566 749 978 4e-08	1.794 015 885e-08	-2.826 461 77e-08	7.033 322 599e-09	-5.186 932 2e-10
$b_7$	-1.651 144 028 4e-10	-2.032 492 61e-10	3.003 151 95e-10	-7.323 652 942e-11	5.294 665 17e-12

### 5 Step 3: Determine the coherent bistatic scattering coefficient

The coherent component of the bistatic scattering coefficient is like polarized component (vv, or hh) and it exists only along the specular reflection direction:

$$\gamma_{pq}^c(\hat{k}_s, \hat{k}_i) = \begin{cases} 4\pi |r_{pp}(\theta_i)|^2 \exp\{-(2k\sigma \cos\theta_i)^2\} & \text{if } \theta_s = \theta_i, \varphi_s = \varphi_i, \text{ and } p = q \\ 0 & \text{otherwise} \end{cases} \quad (11)$$

In the above,  $r_{pp}(\theta_i)$  is Fresnel reflection coefficient for polarization  $p$  ( $p = v, h$ ):

$$r_{hh}(\theta_i) = \frac{\cos\theta_i - \sqrt{\varepsilon_r - \sin^2\theta_i}}{\cos\theta_i + \sqrt{\varepsilon_r - \sin^2\theta_i}} \quad (12)$$

$$r_{vv}(\theta_i) = \frac{\varepsilon_r \cos\theta_i - \sqrt{\varepsilon_r - \sin^2\theta_i}}{\varepsilon_r \cos\theta_i + \sqrt{\varepsilon_r - \sin^2\theta_i}} \quad (13)$$

## 6 Step 4: Determine the diffuse bistatic scattering due to large scale roughness

For getting the bistatic scattering coefficient due to large scale roughness (gravity wave) use the incident angles ( $\theta_i, \varphi_i$ ) and the scattering angles ( $\theta_s, \varphi_s$ ) provided in § 2.1 to calculate the following quantities.

$$q_x = \sin\theta_s \cos\varphi_s - \sin\theta_i \cos\varphi_i \quad (14)$$

$$q_y = \sin\theta_s \sin\varphi_s - \sin\theta_i \sin\varphi_i \quad (15)$$

$$q_z = \cos\theta_s + \cos\theta_i \quad (16)$$

$$q^2 = q_x^2 + q_y^2 + q_z^2 \quad (17)$$

$$(\hat{k}_s \cdot \hat{\nu}_i) = -\sin\theta_s \cos\theta_i \cos(\varphi_s - \varphi_i) - \sin\theta_i \cos\theta_s \quad (18)$$

$$(\hat{k}_s \cdot \hat{h}_i) = \sin\theta_s \sin(\varphi_s - \varphi_i) \quad (19)$$

$$(\hat{k}_i \cdot \hat{\nu}_s) = \sin\theta_i \cos\theta_s \cos(\varphi_s - \varphi_i) + \sin\theta_s \cos\theta_i \quad (20)$$

$$(\hat{k}_i \cdot \hat{h}_s) = -\sin\theta_i \sin(\varphi_s - \varphi_i) \quad (21)$$

$$D_0^2 = (\hat{k}_i \cdot \hat{\nu}_s)^2 + (\hat{k}_i \cdot \hat{h}_s)^2 \quad (22)$$

Introduce equations (16) and (17) into equation (23) to get the local incident angle  $\theta'_i$  at the surface point contributing to the bistatic scattering coefficient:

$$\cos\theta'_i = q |q_z| / (2q_z) \quad (23)$$

Introduce equation (23) into equations (12) and (13) using the proper value of the complex relative permittivity to get local Fresnel reflection  $r'_{hh}$  and  $r'_{vv}$ . Then introduce the local Fresnel coefficients  $r'_{hh}$  and  $r'_{vv}$  along with the scalar vector products of equations (18) to (21) into equations (24) to (27) to get the polarization factors  $U_{pq}(\hat{k}_s, \hat{k}_i)$ 's:

If  $D_0^2 \neq 0$ :

$$U_{hh}(\hat{k}_s, \hat{k}_i) = \{(\hat{k}_s \cdot \hat{\nu}_i)(\hat{k}_i \cdot \hat{\nu}_s)r'_{hh} + (\hat{k}_s \cdot \hat{h}_i)(\hat{k}_i \cdot \hat{h}_s)r'_{vv}\} / D_0^2 \quad (24)$$

$$U_{vh}(\hat{k}_s, \hat{k}_i) = \{-(\hat{k}_s \cdot \hat{\nu}_i)(\hat{k}_i \cdot \hat{h}_s)r'_{hh} + (\hat{k}_s \cdot \hat{h}_i)(\hat{k}_i \cdot \hat{\nu}_s)r'_{vv}\} / D_0^2 \quad (25)$$

$$U_{hv}(\hat{k}_s, \hat{k}_i) = \{-(\hat{k}_s \cdot \hat{h}_i)(\hat{k}_i \cdot \hat{\nu}_s)r'_{hh} + (\hat{k}_s \cdot \hat{\nu}_i)(\hat{k}_i \cdot \hat{h}_s)r'_{vv}\} / D_0^2 \quad (26)$$

$$U_{vv}(\hat{k}_s, \hat{k}_i) = \{(\hat{k}_s \cdot \hat{h}_i)(\hat{k}_i \cdot \hat{h}_s)r'_{hh} + (\hat{k}_s \cdot \hat{\nu}_i)(\hat{k}_i \cdot \hat{\nu}_s)r'_{vv}\} / D_0^2 \quad (27)$$

If  $D_0^2 = 0$ :

$$U_{hh}(\hat{k}_s, \hat{k}_i) = r'_{hh} \quad (28)$$

$$U_{vh}(\hat{k}_s, \hat{k}_i) = 0 \quad (29)$$

$$U_{hv}(\hat{k}_s, \hat{k}_i) = 0 \quad (30)$$

$$U_{vv}(\hat{k}_s, \hat{k}_i) = r'_{vv} \quad (31)$$

Introduce equations (14) to (17) and (24) to (27) into equation (32) to get the sea surface diffuse component of the bistatic scattering coefficient  $\gamma_{pq}^l(\hat{k}_s, \hat{k}_i)$  due to long gravity wave:

$$\gamma_{pq}^l(\hat{k}_s, \hat{k}_i) = \frac{1}{2m_u m_c} \left| \frac{q}{q_z} \right|^4 |U_{pq}(\hat{k}_s, \hat{k}_i)|^2 \exp \left\{ \frac{-1}{2q_z^2} \left( \left\{ \frac{q_x}{m_u} \right\}^2 + \left\{ \frac{q_y}{m_c} \right\}^2 \right) \right\} \quad (32)$$

where  $m_u$  and  $m_c$  are the upwind and the crosswind mean squared surface slopes given in equations (7) and (8) as a function of wind speed  $U_{10}$  and frequency  $f$ .

## 7 Step 5: Determine the diffuse bistatic scattering due to small-scale roughness

The approach exploited in getting the diffuse bistatic scattering due to small-scale roughness starts by setting the maxima and minima of  $S_u$  and  $S_c$ .

$$S_{u,max} = 6 m_u$$

$$S_{u,min} = -\min(6 m_u, \cot \theta_i)$$

$$S_{c,max} = 6 m_c$$

$$S_{c,min} = -6 m_c$$

The slope region subtended by the above maxima and minima are divided into  $64 \times 64$  points using Gaussian quadrature nodes. At an arbitrary node  $(t, m)$  the slopes can be written as:

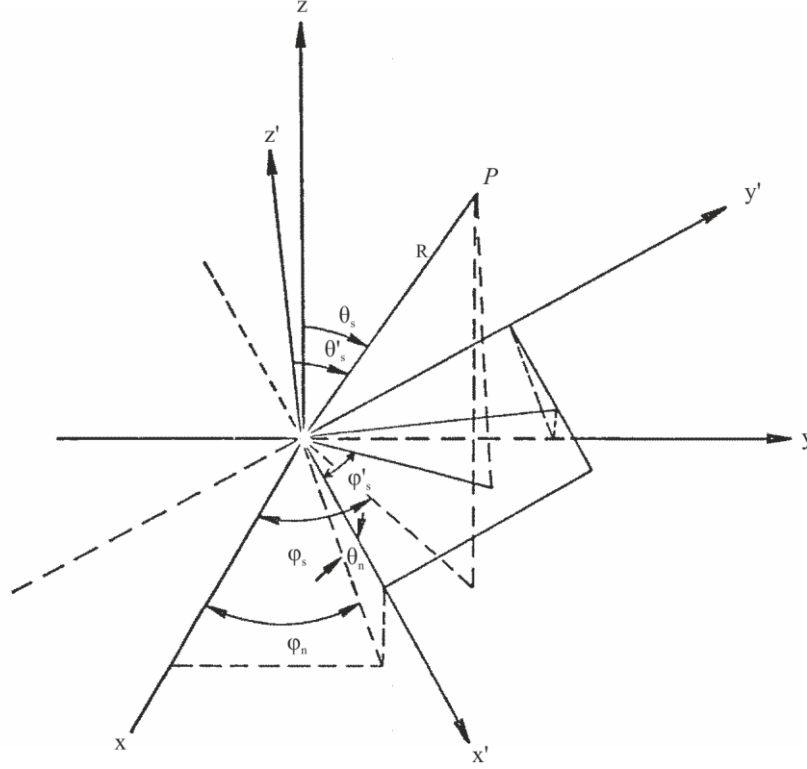
$$S_{u,t} = \frac{1}{2} \{ (S_{u,max} - S_{u,min}) \chi(t) + (S_{u,max} + S_{u,min}) \} \quad (33)$$

$$S_{c,m} = \frac{1}{2} \{ (S_{c,max} - S_{c,min}) \zeta(m) + (S_{c,max} + S_{c,min}) \} \quad (34)$$

In equations (33) and (34),  $\chi(t)$  and  $\zeta(m)$  are the Gaussian Quadrature nodes ( $t, m = 1, \dots, 64$ ) which correspond to the  $X_i$  of Section 3 of the Annex to Recommendation ITU-R P.1144-11, i.e.  $\chi(t), \zeta(m) \rightarrow X_i$ . Also  $S_{u,t} \rightarrow X'_i$  and  $S_{c,m} \rightarrow Z'_i$ .

FIGURE 4

Local scattering angles ( $\theta'_s, \varphi'_s$ ) and inclination angles of surface normal (zenith angle  $\theta_n$  and azimuth angle  $\varphi_n$ )



P.2146-04

At the above Gaussian node perform the following procedures:

- Get the zenith angle  $\theta_n$  and azimuth angle  $\varphi_n$  defining the inclination of the sea surface large-scale surface normal  $\hat{n}$  (see Fig. 4) through introducing equations (32) and (33) into equations (35) to (37):

$$\varphi_n = \tan^{-1}\{S_{c,m}/S_{u,t}\} \quad (35)$$

$$\cos \theta_n = \frac{1}{\sqrt{S_{u,t}^2 + S_{c,m}^2 + 1}} \quad (36)$$

$$\sin \theta_n = \cos \theta_n \{S_{u,t} \cos \varphi_n + S_{c,m} \sin \varphi_n\} \quad (37)$$

- Get the local scattering and incident angles  $\theta'_s$ , and  $\varphi'_s$ , and  $\theta'_i$ , and  $\varphi'_i$  at this node point:

$$\varphi'_s = \tan^{-1} \left\{ \frac{\sin \theta_s \sin(\varphi_s - \varphi_n)}{\sin \theta_s \cos \theta_n \cos(\varphi_s - \varphi_n) + \cos \theta_s \sin \theta_n} \right\} \quad (38)$$

$$\cos \theta'_s = \frac{\{-\sin \theta_s (S_{u,t} \cos \varphi_s + S_{c,m} \sin \varphi_s) + \cos \theta_s\}}{\sqrt{S_{u,t}^2 + S_{c,m}^2 + 1}} \quad (39)$$

$$\sin \theta'_s = \{\sin \theta_s \cos \theta_n \cos(\varphi_s - \varphi_n) + \cos \theta_s \sin \theta_n\} \cos \varphi'_s + \{\sin \theta_s \sin(\varphi_s - \varphi_n)\} \sin \varphi'_s \quad (40)$$

and

$$\varphi'_i = \tan^{-1} \left\{ \frac{\sin \theta_i \sin(\varphi_i - \varphi_n)}{\sin \theta_i \cos \theta_n \cos(\varphi_i - \varphi_n) - \cos \theta_i \sin \theta_n} \right\} \quad (41)$$

$$\cos \theta'_i = \frac{\{\sin \theta_i (S_{u,t} \cos \varphi_i + S_{c,m} \sin \varphi_i) + \cos \theta_i\}}{\sqrt{S_{u,t}^2 + S_{c,m}^2 + 1}} \quad (42)$$

$$\sin \theta'_i = \{\sin \theta_i \cos \theta_n \cos(\varphi_i - \varphi_n) - \cos \theta_i \sin \theta_n\} \cos \varphi'_i + \{\sin \theta_i \sin(\varphi_i - \varphi_n)\} \sin \varphi'_i \quad (43)$$

– Get the local incident and scattered angles enables getting the components of the incident horizontal polarization and scattered horizontal polarization:

$$h_{xi} = \sin \theta_i \sin \varphi_i - \cos \theta_i S_{c,m} \quad (44)$$

$$h_{yi} = \cos \theta_i S_{u,t} - \sin \theta_i \cos \varphi_i \quad (45)$$

$$h_{zi} = \sin \theta_i (S_{u,t} \sin \varphi_i - S_{c,m} \cos \varphi_i) \quad (46)$$

$$D_i = \sqrt{h_{xi}^2 + h_{yi}^2 + h_{zi}^2} \quad (47)$$

and

$$h_{xs} = \sin \theta_s \sin \varphi_s + \cos \theta_s S_{c,m} \quad (48)$$

$$h_{ys} = -\{\cos \theta_s S_{u,t} + \sin \theta_s \cos \varphi_s\} \quad (49)$$

$$h_{zs} = \sin \theta_s (S_{u,t} \sin \varphi_s - S_{c,m} \cos \varphi_s) \quad (50)$$

$$D_s = \sqrt{h_{xs}^2 + h_{ys}^2 + h_{zs}^2} \quad (51)$$

– Get the following scalar vector products in the incident direction:

$$(\vartheta'_i \cdot \vartheta_i) = \cos \theta_n \{-\cos \theta_i (S_{u,t} \cos \varphi_i + S_{c,m} \sin \varphi_i) + \sin \theta_i\} / D_i \quad (52)$$

$$(\vartheta'_i \cdot \hat{h}_i) = \cos \theta_n \{-S_{u,t} \sin \varphi_i + S_{c,m} \cos \varphi_i\} / D_i \quad (53)$$

$$(\hat{h}'_i \cdot \vartheta_i) = \frac{-1}{D_i} \{\cos \theta_i (h_{xi} \cos \varphi_i + h_{yi} \sin \varphi_i) + h_{zi} \sin \theta_i\} \quad (54)$$

$$(\hat{h}'_i \cdot \hat{h}_i) = \frac{1}{D_i} \{h_{yi} \cos \varphi_i - h_{xi} \sin \varphi_i\} \quad (55)$$

And the following scalar vector products in the scattering direction:

$$(\vartheta'_s \cdot \vartheta'_s) = \cos \theta_n \{\cos \theta_s (S_{u,t} \cos \varphi_s + S_{c,m} \sin \varphi_s) + \sin \theta_s\} / D_s \quad (56)$$

$$(\vartheta'_s \cdot \hat{h}'_s) = \frac{1}{D_s} \{\cos \theta_s (h_{xs} \cos \varphi_s + h_{ys} \sin \varphi_s) - h_{zs} \sin \theta_s\} \quad (57)$$

$$(\hat{h}'_s \cdot \vartheta'_s) = \cos \theta_n \{-S_{u,t} \sin \varphi_s + S_{c,m} \cos \varphi_s\} / D_s \quad (58)$$

$$(\hat{h}'_s \cdot \hat{h}'_s) = \frac{1}{D_s} \{h_{ys} \cos \varphi_s - h_{xs} \sin \varphi_s\} \quad (59)$$

– Get the polarization factors in the local frame  $g'_{pq}$  's through introducing equations (38) and (41) along with proper value of complex relative permittivity into equations (60) to (63):

$$g'_{hh} = \frac{(\varepsilon_r - 1)}{\left(\cos \theta'_s + \sqrt{\varepsilon_r - \sin^2 \theta'_s}\right) \left(\cos \theta'_i + \sqrt{\varepsilon_r - \sin^2 \theta'_i}\right)} \cos(\varphi'_s - \varphi'_i) \quad (60)$$

$$g'_{vh} = \frac{-(\varepsilon_r - 1) \sqrt{\varepsilon_r - \sin^2 \theta'_s}}{\left(\varepsilon_r \cos \theta'_s + \sqrt{\varepsilon_r - \sin^2 \theta'_s}\right) \left(\cos \theta'_i + \sqrt{\varepsilon_r - \sin^2 \theta'_i}\right)} \sin(\varphi'_s - \varphi'_i) \quad (61)$$

$$g'_{hv} = \frac{(\varepsilon_r - 1) \sqrt{\varepsilon_r - \sin^2 \theta'_i}}{\left(\cos \theta'_s + \sqrt{\varepsilon_r - \sin^2 \theta'_s}\right) \left(\varepsilon_r \cos \theta'_i + \sqrt{\varepsilon_r - \sin^2 \theta'_i}\right)} \sin(\varphi'_s - \varphi'_i) \quad (62)$$



$$g'_{vv} = \frac{(\varepsilon_r - 1) \left( \varepsilon_r \sin \theta'_i \sin \theta'_s - \sqrt{\varepsilon_r - \sin^2 \theta'_s} \sqrt{\varepsilon_r - \sin^2 \theta'_i} \cos(\varphi'_s - \varphi'_i) \right)}{\left( \varepsilon_r \cos \theta'_s + \sqrt{\varepsilon_r - \sin^2 \theta'_s} \right) \left( \varepsilon_r \cos \theta'_i + \sqrt{\varepsilon_r - \sin^2 \theta'_i} \right)} \quad (63)$$

– Get the polarization factors  $G_{pq}$ 's through introducing equations (60) to (63), and equations (52) to (59) into equations (64) to (67):

$$G_{vv} = \{(\vartheta_s \cdot \vartheta'_s)g'_{vv} + (\vartheta_s \cdot \hat{h}'_s)g'_{hv}\}(\vartheta'_i \cdot \vartheta_i) + \{(\vartheta_s \cdot \vartheta'_s)g'_{vh} + (\vartheta_s \cdot \hat{h}'_s)g'_{hh}\}(\hat{h}'_i \cdot \vartheta_i) \quad (64)$$

$$G_{vh} = \{(\vartheta_s \cdot \vartheta'_s)g'_{vv} + (\vartheta_s \cdot \hat{h}'_s)g'_{hv}\}(\vartheta'_i \cdot \hat{h}_i) + \{(\vartheta_s \cdot \vartheta'_s)g'_{vh} + (\vartheta_s \cdot \hat{h}'_s)g'_{hh}\}(\hat{h}'_i \cdot \hat{h}_i) \quad (65)$$

$$G_{hv} = \{(\hat{h}_s \cdot \vartheta'_s)g'_{vv} + (\hat{h}_s \cdot \hat{h}'_s)g'_{hv}\}(\vartheta'_i \cdot \vartheta_i) + \{(\hat{h}_s \cdot \vartheta'_s)g'_{vh} + (\hat{h}_s \cdot \hat{h}'_s)g'_{hh}\}(\hat{h}'_i \cdot \vartheta_i) \quad (66)$$

$$G_{hh} = \{(\hat{h}_s \cdot \vartheta'_s)g'_{vv} + (\hat{h}_s \cdot \hat{h}'_s)g'_{hv}\}(\vartheta'_i \cdot \hat{h}_i) + \{(\hat{h}_s \cdot \vartheta'_s)g'_{vh} + (\hat{h}_s \cdot \hat{h}'_s)g'_{hh}\}(\hat{h}'_i \cdot \hat{h}_i) \quad (67)$$

The function  $\mathcal{U}$  ensures that the Gaussian node  $(t, m)$  sees the incident direction and scattered direction simultaneously:

$$\mathcal{U}(S_{u,t}, \theta_i) = \begin{cases} \max((1 + S_{u,t} \tan \theta_i), 0) & \text{if } 0 \leq \theta'_i \leq \frac{\pi}{2} \text{ and } 0 \leq \theta'_s \leq \frac{\pi}{2} \\ 0 & \text{otherwise} \end{cases} \quad (68)$$

The above procedures need to be repeated to cover all the nodes of the slope.

To get sea surface diffuse bistatic scattering coefficient due to short waves, use the above formulations to calculate (69) and (70) at all nodes:

$$P(S_{u,t}, S_{c,m}) = \frac{1}{2\pi m_u m_c} \exp\left\{-\frac{1}{2} \left( \frac{S_{u,t}^2}{m_u^2} + \frac{S_{c,m}^2}{m_c^2} \right)\right\} \quad (69)$$

$$\gamma_{pq}^{cap}(\hat{k}_s, \hat{k}_i) = 16\pi(k^2 \cos \theta'_s \cos \theta'_i)^2 |G_{pq}|^2 W_s(\kappa, \varphi_i) \quad (70)$$

Equation (69) is obtained from equation (6). In addition,  $W_s(\kappa, \varphi_i)$  in equation (70) is the short-wave spectral density function given in Attachment D calculated at  $\psi = \varphi_i$ , and height wavenumber  $\kappa$  given by:

$$\kappa = k \sqrt{\sin^2 \theta'_s + \sin^2 \theta'_i - 2 \sin \theta'_s \sin \theta'_i \cos(\varphi'_s - \varphi'_i)} \quad (71)$$

Then introduce equations (68) to (71) into equation (72) to get the sea surface diffuse bistatic scattering coefficient due to small-scale roughness (short capillary wave):

$$\gamma_{pq}^s(\hat{k}_s, \hat{k}_i) = C \sum_{m=1}^{64} \sum_{t=1}^{64} \gamma_{pq}^{cap}(\hat{k}_s, \hat{k}_i) \mathcal{U}(S_{u,t}, \theta_i) P(S_{u,t}, S_{c,m}) w_{u,t} w_{c,m} \quad (72)$$

In equation (72),  $w_{u,t}$  and  $w_{c,m}$  are the Gaussian quadrature weights which are given in Section 3 of the Annex to Recommendation ITU-R P.1144-11. The factor  $C$  is a constant given by:

$$C = \frac{1}{4} \{(S_{u,max} - S_{u,min})(S_{c,max} - S_{c,min})\} \quad (73)$$

## 8 Sum the components of sea surface bistatic scattering coefficient

The coherent component (11) and diffuse components (32) and (72) of sea surface bistatic scattering coefficients are summed and exploited in exploring features of those coefficients in the backscattering direction and the forward (specular) direction.

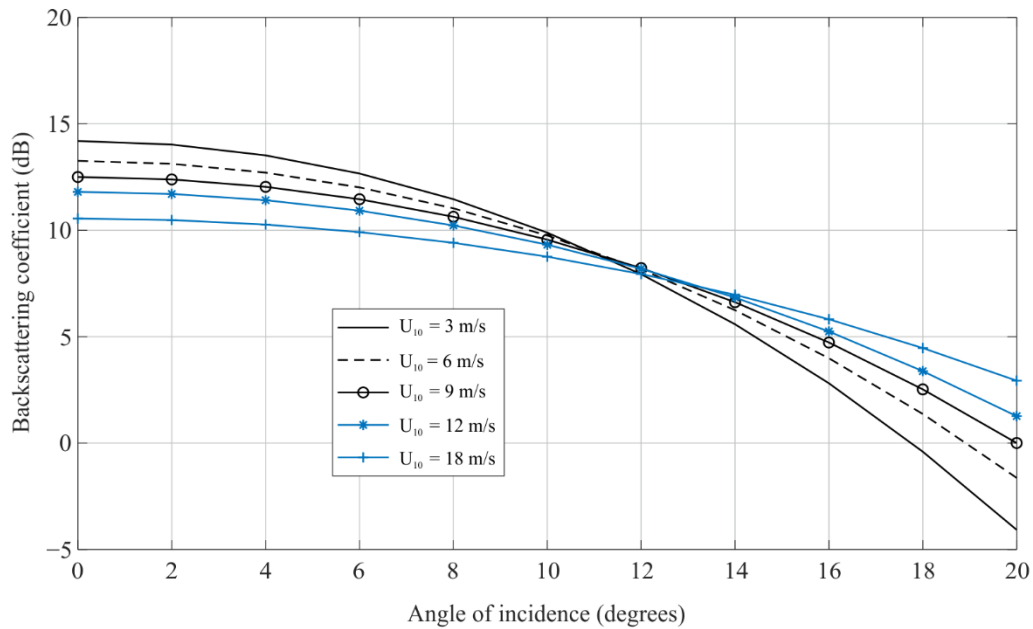
$$\gamma_{pq}^s(\hat{k}_s, \hat{k}_i) = \gamma_{pq}^l(\hat{k}_s, \hat{k}_i) + \gamma_{pq}^s(\hat{k}_s, \hat{k}_i) + \gamma_{pq}^c(\hat{k}_s, \hat{k}_i) \quad (74)$$

### 8.1 Sea surface backscattering coefficients

The sea surface backscattering coefficients are of interest, especially to the active remote sensing communities. They have no coherent component, and they can be calculated from the sum of equations (32) and (72) by setting  $\hat{k}_s = -\hat{k}_i$  (i.e.  $\theta_s = \theta_i$ , and  $\varphi_s = \pi + \varphi_i$ ). Figures 5 to 8 illustrate the dependence of the sea surface backscattering coefficients on incidence angle, polarization, wind speed and wind direction.

FIGURE 5

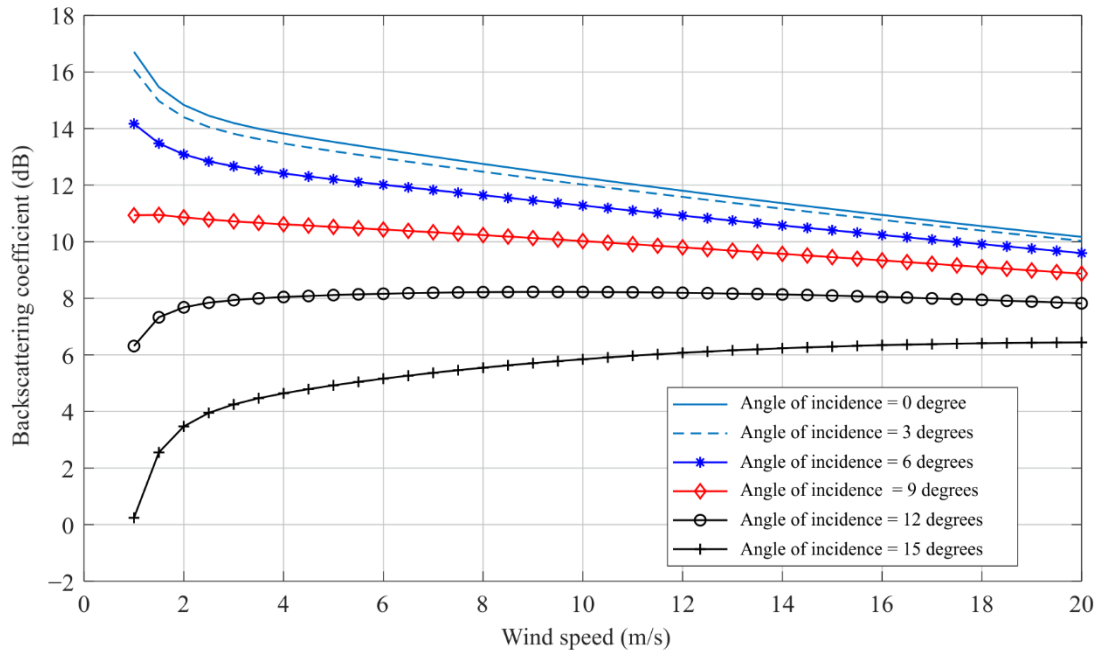
**Backscattering coefficients along upwind direction as a function of incidence angle at different values of wind speed (frequency = 13.6 GHz,  $\Omega = 0.84$ , temperature = 30° C, salinity = 35 ppt)**



P.2146-05

FIGURE 6

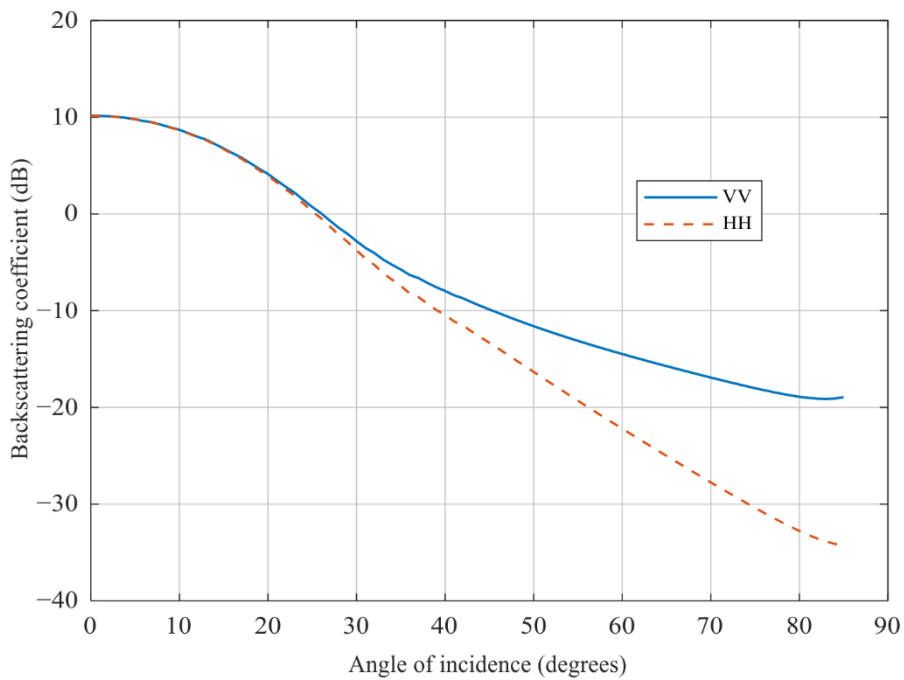
**Backscattering coefficients as a function of wind speed at different angles of incidence**  
 (frequency = 13.6 GHz,  $\Omega = 0.84$ , temperature = 30° C, salinity = 35 ppt)



P.2146-06

FIGURE 7

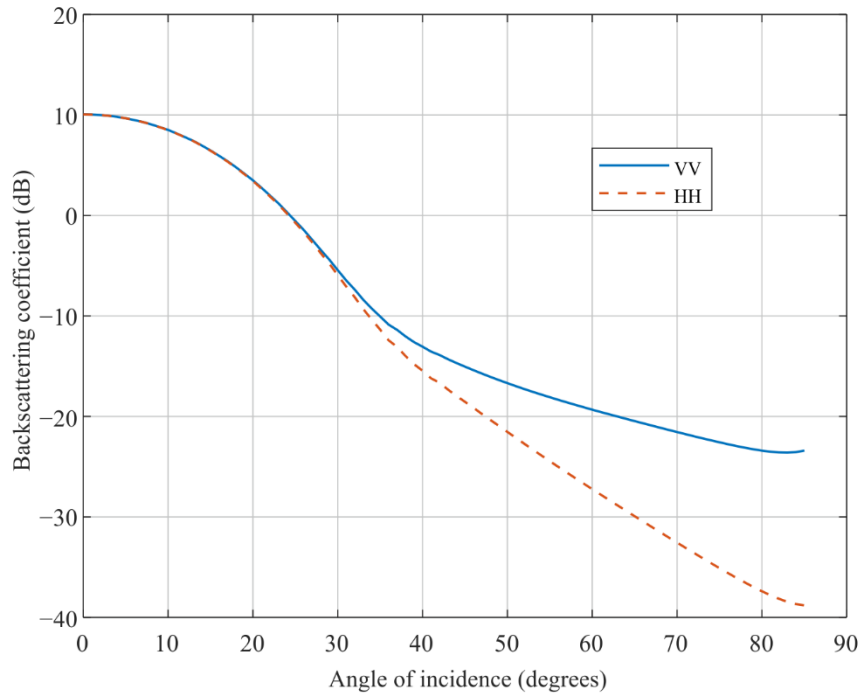
**Upwind backscattering coefficients as a function of incidence angle**  
 (frequency = 18.6 GHz,  $\Omega = 0.84$ , temperature = 30° C,  $U_{10} = 18$  m/s, salinity = 35 ppt)



P.2146-07

FIGURE 8

Crosswind backscattering coefficients as a function of incidence angle  
(frequency = 18.6 GHz,  $\Omega = 0.84$ , temperature = 30° C,  $U_{10} = 18$  m/s, salinity = 35 ppt)



P.2146-08

## 8.2 Sea surface bistatic scattering coefficients in the forward direction

The sea surface bistatic scattering coefficients in the forward direction can be used for assessing the interference power received by a receive antenna. These sea surface bistatic scattering coefficients can also be used to calculate the fading depth due to sea surface reflections in Recommendation ITU-R P.680-3. They can be calculated as the sum of the coherent component (11) and the diffuse components. The coherent component exists only along the specular reflection direction ( $\theta_s = \theta_i$ , and  $\varphi_s = \varphi_i$ ). The diffuse component is defined in equations (32) and (72) by setting  $\theta_s = \theta_i \wedge \varphi_s = \varphi_i$ .

Figures 9 to 14 are examples of the bistatic scattering coefficients in the forward direction. Figures 9 and 10 fix the scattering angle (the receive observation angle) and vary the angle of incidence (direction of the interfering signals). Figure 9 is calculated at 1.227 6 GHz (GPS L2 frequency), and Fig. 10 is calculated at 18.6 GHz. In each Figure, the bistatic scattering coefficients are calculated at two different wind speeds:  $U_{10} = 2$  m/s, and  $U_{10} = 25$  m/s.

Figures 11 to 14 fix the incidence angle (interferer angle) and vary the scattering angle. Figures 11 and 13 are calculated at 1.227 6 GHz, and Figs 12 and 14 are calculated at 18.6 GHz. Figures 11 and 12 are calculated at sea surface temperature of 30° C. Figures 13 and 14 are calculated at a sea surface temperature of 5° C. Moreover, in each of Figs 11 to 14, the bistatic scattering coefficients are calculated at two different wind speeds:  $U_{10} = 2$  m/s, and  $U_{10} = 25$  m/s.

Due to reciprocity, fixing either the angle of incidence or the scattering angle yields similar results. Accordingly, the fixed value of scattering angle in Figs 8 and 9 are different than the fixed value of the incident angle in Figs 11 to 14.

Comparing Fig. 11 against Fig. 13 and comparing Fig. 12 against Fig. 14 indicate that for temperature above freezing condition, the temperature has no pronounced effect on the bistatic scattering coefficient.

FIGURE 9

Forward bistatic scattering coefficients as a function of incidence angle at different values of wind speeds ( $\theta_s = 30^\circ$ , frequency = 1.227 6 GHz,  $\Omega = 0.84$ , temperature = 30° C, salinity = 35 ppt)

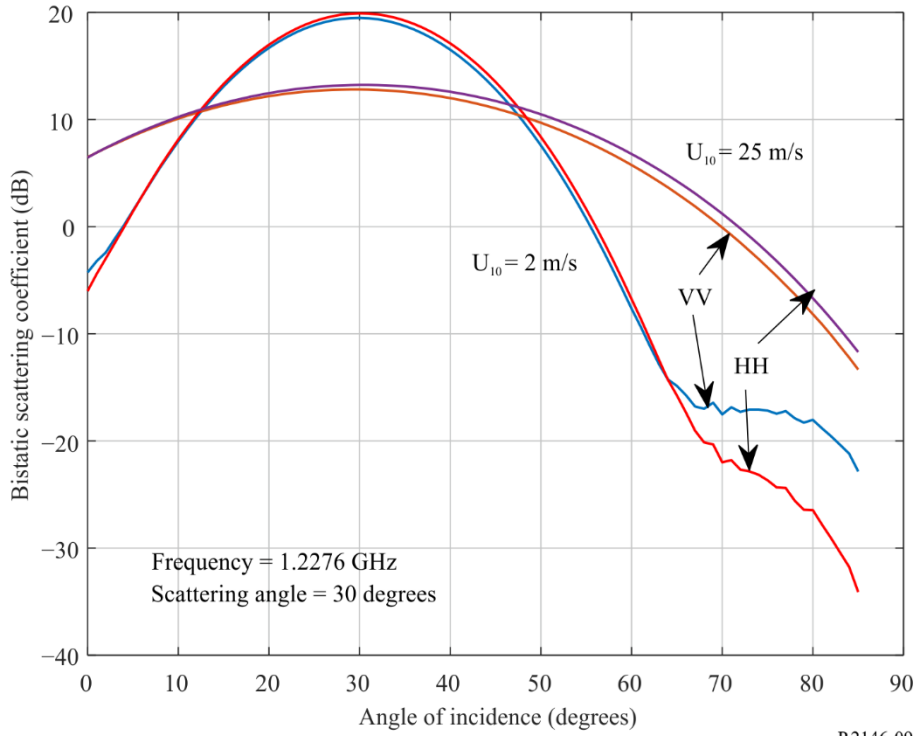


FIGURE 10

Forward bistatic scattering coefficients as a function of incidence angle at different values of wind speeds ( $\theta_s = 30^\circ$ , frequency = 18.6 GHz,  $\Omega = 0.84$ , temperature = 30° C, salinity = 35 ppt)

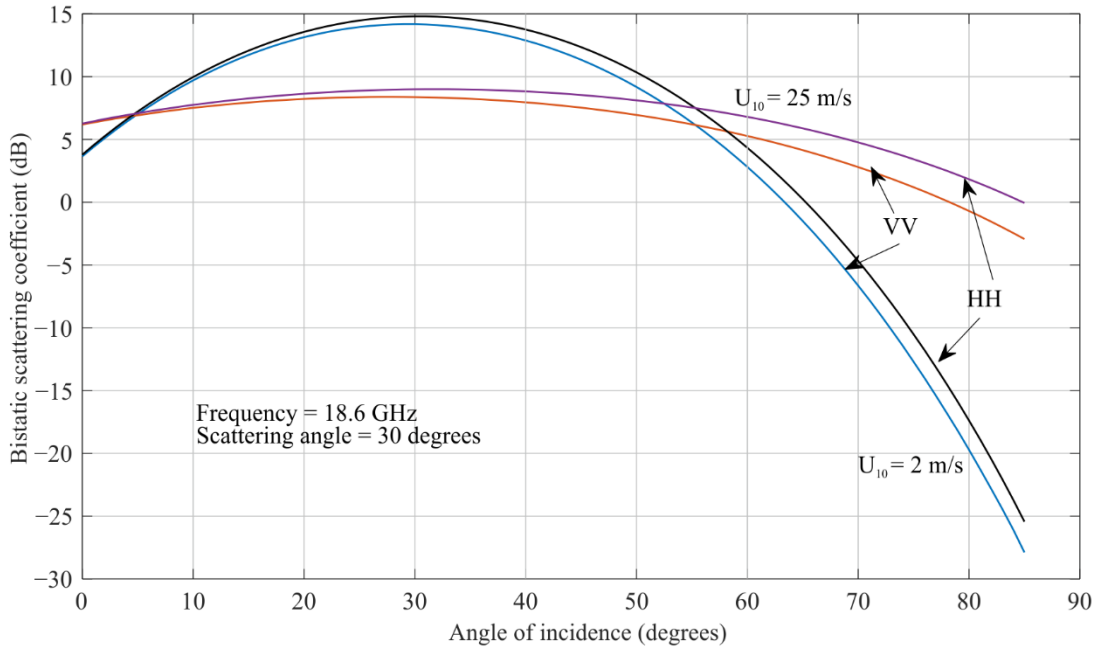
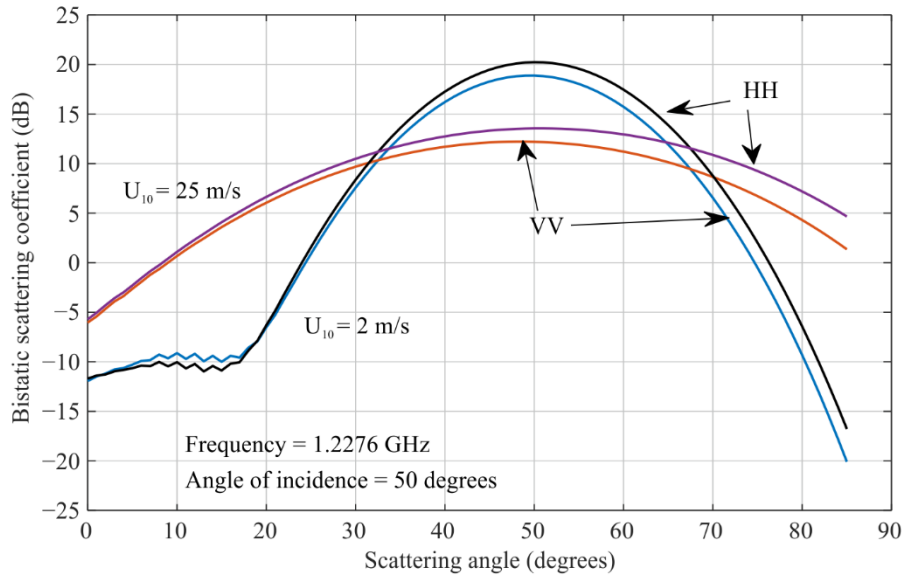


FIGURE 11

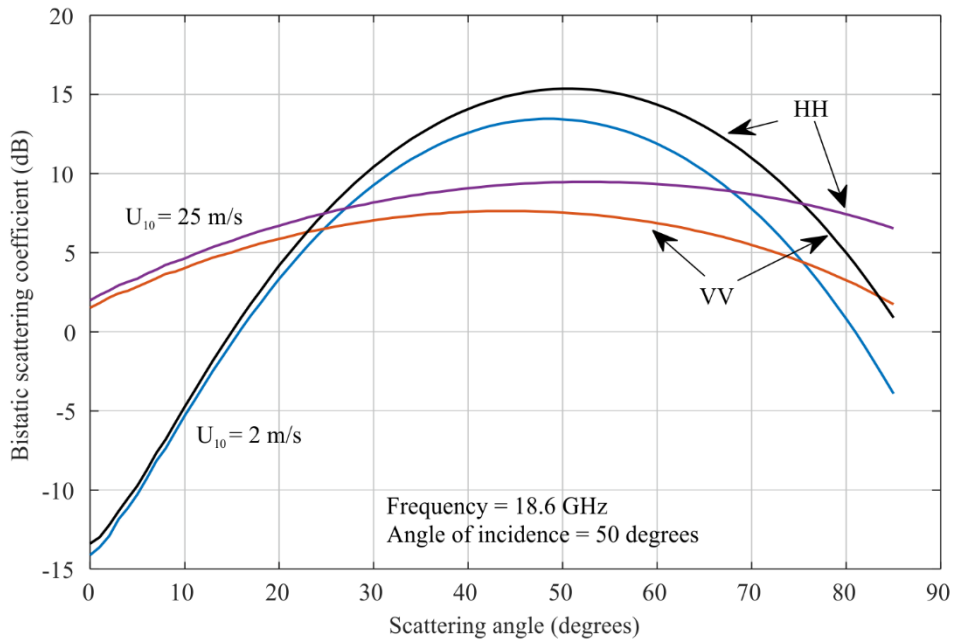
Forward bistatic scattering coefficients as a function of scattering angle at different values of wind speeds ( $\theta_i = 50^\circ$ , frequency = 1.227 6 GHz,  $\Omega = 0.84$ , temperature = 30 °C, salinity = 35 ppt)



P.2146-11

FIGURE 12

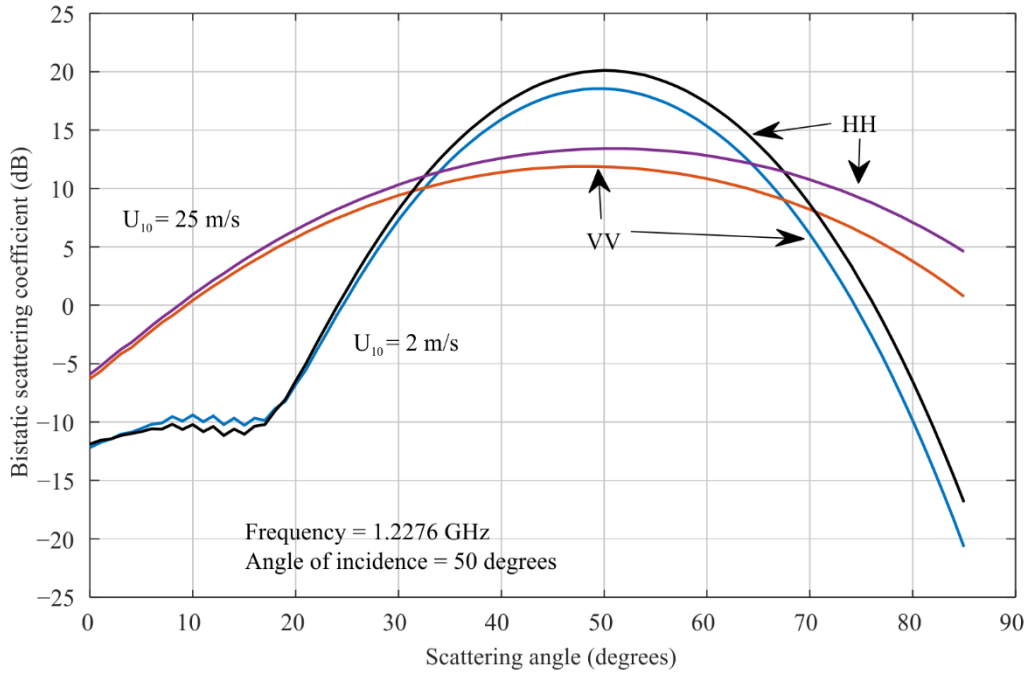
Forward bistatic scattering coefficients as a function of scattering angle at different values of wind speeds ( $\theta_i = 50^\circ$ , frequency = 18.6 GHz,  $\Omega = 0.84$ , temperature = 30 °C, salinity = 35 ppt)



P.2146-12

FIGURE 13

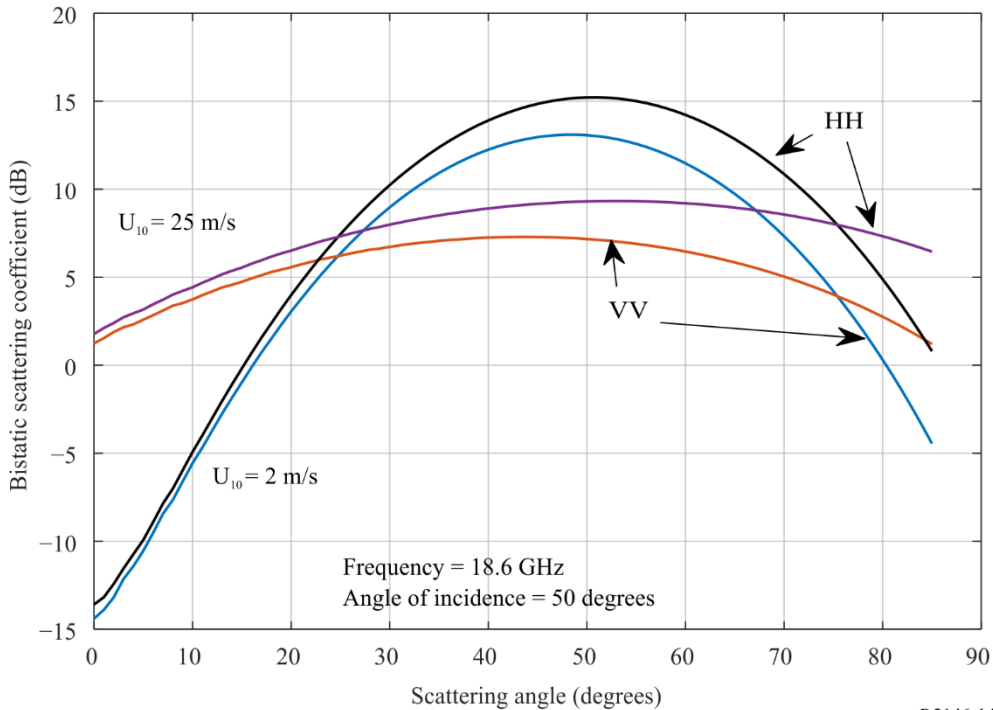
Forward bistatic scattering coefficients as a function of scattering angle at different values of wind speeds ( $\theta_i = 50^\circ$ , frequency = 1.227 6 GHz,  $\Omega = 0.84$ , temperature =  $5^\circ$  C, salinity = 35 ppt)



P.2146-13

FIGURE 14

Forward bistatic scattering coefficients as a function of scattering angle at different values of wind speeds ( $\theta_i = 50^\circ$ , frequency = 18.6 GHz,  $\Omega = 0.84$ , temperature =  $5^\circ$  C, salinity = 35 ppt)



P.2146-14

## Attachment A to Annex

### Calculation of scattering coefficients between circularly polarized and linearly polarized waves

This Attachment provides the calculations of the bistatic scattering coefficients between a) a circularly polarized incident wave and a linearly polarized scattered wave (i.e.  $\gamma_{qc}$ , where  $c$  is either right-hand circular polarization,  $R$ , or left-hand circular polarization,  $L$ , and  $q$  is either vertical,  $v$ , or horizontal,  $h$ , polarization) and b) a linearly polarized incident wave and a circularly polarized scattered wave (i.e.  $\gamma_{cq}$ , where  $q$  is either vertical,  $v$ , or horizontal,  $h$ , polarization and  $c$  is either right-hand circular polarization,  $R$ , or left-hand circular polarization,  $L$ ).

#### A.1 Circularly Polarized (CP) incident to linear scattered power

In this case, the coherent bistatic scattering coefficient  $\gamma_{pc}^c(\hat{k}_s, \hat{k}_i)$  components due to sea surface can be obtained from equation (11) through replacing  $r_{pp}(\theta_i)$  by  $r_{pc}(\theta_i)$  with

$$r_{vR}(\theta_i) = \frac{1}{\sqrt{2}} r_{vv}(\theta_i) \quad (\text{a.1})$$

$$r_{hR}(\theta_i) = \frac{-j}{\sqrt{2}} r_{hh}(\theta_i) \quad (\text{a.2})$$

$$r_{vL}(\theta_i) = \frac{1}{\sqrt{2}} r_{vv}(\theta_i) \quad (\text{a.3})$$

$$r_{hL}(\theta_i) = \frac{j}{\sqrt{2}} r_{hh}(\theta_i) \quad (\text{a.4})$$

$$\text{and } j = \sqrt{-1}.$$

The bistatic scattering coefficient  $\gamma_{pc}^l(\hat{k}_s, \hat{k}_i)$  due to long gravity wave can be obtained from equation (32) through replacing the polarization factors  $U_{pq}(\hat{k}_s, \hat{k}_i)$  by the polarization factors  $U_{pc}(\hat{k}_s, \hat{k}_i)$  with:

$$U_{vR}(\hat{k}_s, \hat{k}_i) = \frac{1}{\sqrt{2}} \{U_{vv}(\hat{k}_s, \hat{k}_i) - jU_{vh}(\hat{k}_s, \hat{k}_i)\} \quad (\text{a.5})$$

$$U_{hR}(\hat{k}_s, \hat{k}_i) = \frac{1}{\sqrt{2}} \{U_{hv}(\hat{k}_s, \hat{k}_i) - jU_{hh}(\hat{k}_s, \hat{k}_i)\} \quad (\text{a.6})$$

$$U_{vL}(\hat{k}_s, \hat{k}_i) = \frac{1}{\sqrt{2}} \{U_{vv}(\hat{k}_s, \hat{k}_i) + jU_{vh}(\hat{k}_s, \hat{k}_i)\} \quad (\text{a.7})$$

$$U_{hL}(\hat{k}_s, \hat{k}_i) = \frac{1}{\sqrt{2}} \{U_{hv}(\hat{k}_s, \hat{k}_i) + jU_{hh}(\hat{k}_s, \hat{k}_i)\} \quad (\text{a.8})$$

The bistatic scattering coefficient  $\gamma_{pc}^{sh}(\hat{k}_s, \hat{k}_i)$  due to short capillary wave can be obtained from equation (72) through replacing the polarization factors  $G_{pq}(\hat{k}_s, \hat{k}_i)$  in equation (70) by the polarization factors  $G_{pc}(\hat{k}_s, \hat{k}_i)$  with:

$$G_{vR}(\hat{k}_s, \hat{k}_i) = \frac{1}{\sqrt{2}} \{G_{vv}(\hat{k}_s, \hat{k}_i) - jG_{vh}(\hat{k}_s, \hat{k}_i)\} \quad (\text{a.9})$$

$$G_{hR}(\hat{k}_s, \hat{k}_i) = \frac{1}{\sqrt{2}} \{G_{hv}(\hat{k}_s, \hat{k}_i) - jG_{hh}(\hat{k}_s, \hat{k}_i)\} \quad (\text{a.10})$$

$$G_{vL}(\hat{k}_s, \hat{k}_i) = \frac{1}{\sqrt{2}} \{G_{vv}(\hat{k}_s, \hat{k}_i) + jG_{vh}(\hat{k}_s, \hat{k}_i)\} \quad (\text{a.11})$$

$$G_{hL}(\hat{k}_s, \hat{k}_i) = \frac{1}{\sqrt{2}} \{G_{hv}(\hat{k}_s, \hat{k}_i) + jG_{hh}(\hat{k}_s, \hat{k}_i)\} \quad (\text{a.12})$$



## A.2 Linear incident to CP scattered power

For this case, the coherent bistatic scattering coefficient  $\gamma_{cq}^c(\hat{k}_s, \hat{k}_i)$  components due to sea surface can be obtained from equation (11) through replacing  $r_{pp}(\theta_i)$  by  $r_{cq}(\theta_i)$  with:

$$r_{Rv}(\theta_i) = \frac{1}{\sqrt{2}} r_{vv}(\theta_i) \quad (\text{a.13})$$

$$r_{Lv}(\theta_i) = \frac{1}{\sqrt{2}} r_{vv}(\theta_i) \quad (\text{a.14})$$

$$r_{Rh}(\theta_i) = \frac{j}{\sqrt{2}} r_{hh}(\theta_i) \quad (\text{a.15})$$

$$r_{Lh}(\theta_i) = \frac{-j}{\sqrt{2}} r_{hh}(\theta_i) \quad (\text{a.16})$$

The bistatic scattering coefficient  $\gamma_{cq}^l(\hat{k}_s, \hat{k}_i)$  due to long gravity wave can be obtained from equation (32) through replacing  $U_{pq}(\hat{k}_s, \hat{k}_i)$  by  $U_{cq}(\hat{k}_s, \hat{k}_i)$  with:

$$U_{Rv}(\hat{k}_s, \hat{k}_i) = \frac{1}{\sqrt{2}} \{U_{vv}(\hat{k}_s, \hat{k}_i) + jU_{hv}(\hat{k}_s, \hat{k}_i)\} \quad (\text{a.17})$$

$$U_{Lv}(\hat{k}_s, \hat{k}_i) = \frac{1}{\sqrt{2}} \{U_{vv}(\hat{k}_s, \hat{k}_i) - jU_{hv}(\hat{k}_s, \hat{k}_i)\} \quad (\text{a.18})$$

$$U_{Rh}(\hat{k}_s, \hat{k}_i) = \frac{1}{\sqrt{2}} \{U_{vh}(\hat{k}_s, \hat{k}_i) + jU_{hh}(\hat{k}_s, \hat{k}_i)\} \quad (\text{a.19})$$

$$U_{Lh}(\hat{k}_s, \hat{k}_i) = \frac{1}{\sqrt{2}} \{U_{vh}(\hat{k}_s, \hat{k}_i) - jU_{hh}(\hat{k}_s, \hat{k}_i)\} \quad (\text{a.20})$$

The bistatic scattering coefficient  $\gamma_{cq}^s(\hat{k}_s, \hat{k}_i)$  due to short capillary wave can be obtained from equation (72) through replacing  $G_{pq}(\hat{k}_s, \hat{k}_i)$  in equation (70) by  $G_{cq}(\hat{k}_s, \hat{k}_i)$  with:

$$G_{Rv}(\hat{k}_s, \hat{k}_i) = \frac{1}{\sqrt{2}} \{G_{vv}(\hat{k}_s, \hat{k}_i) + jG_{hv}(\hat{k}_s, \hat{k}_i)\} \quad (\text{a.21})$$

$$G_{Lv}(\hat{k}_s, \hat{k}_i) = \frac{1}{\sqrt{2}} \{G_{vv}(\hat{k}_s, \hat{k}_i) - jG_{hv}(\hat{k}_s, \hat{k}_i)\} \quad (\text{a.22})$$

$$G_{Rh}(\hat{k}_s, \hat{k}_i) = \frac{1}{\sqrt{2}} \{G_{vh}(\hat{k}_s, \hat{k}_i) + jG_{hh}(\hat{k}_s, \hat{k}_i)\} \quad (\text{a.23})$$

$$G_{Lh}(\hat{k}_s, \hat{k}_i) = \frac{1}{\sqrt{2}} \{G_{vh}(\hat{k}_s, \hat{k}_i) - jG_{hh}(\hat{k}_s, \hat{k}_i)\} \quad (\text{a.24})$$

## Attachment B to Annex

### Calculation of scattering coefficients between circularly polarized waves

This Attachment provides the calculations of the bistatic scattering coefficients between a circularly polarized incident wave and a circularly polarized scattered wave (i.e.  $\gamma_{PQ}$ , where  $P$  is either right-hand circular polarization,  $R$ , or left-hand circular polarization,  $L$ , and  $Q$  is either right-hand circular polarization,  $R$ , or left-hand circular polarization,  $L$ ).

The coherent bistatic scattering coefficient  $\gamma_{cc}^c(\hat{k}_s, \hat{k}_i)$  components due to sea surface can be obtained from equation (11) through replacing  $r_{pp}(\theta_i)$  by  $r_{PQ}(\theta_i)$  with:

$$r_{RR}(\theta_i) = \frac{1}{2} \{r_{vv}(\theta_i) + r_{hh}(\theta_i)\} \quad (\text{b.1})$$

$$r_{RL}(\theta_i) = \frac{1}{2} \{r_{vv}(\theta_i) - r_{hh}(\theta_i)\} \quad (\text{b.2})$$

$$r_{LR}(\theta_i) = \frac{1}{2} \{r_{vv}(\theta_i) - r_{hh}(\theta_i)\} \quad (\text{b.3})$$

$$r_{LL}(\theta_i) = \frac{1}{2} \{r_{vv}(\theta_i) + r_{hh}(\theta_i)\} \quad (\text{b.4})$$

The bistatic scattering coefficient  $\gamma_{PQ}^l(\hat{k}_s, \hat{k}_i)$  due to long gravity wave can be obtained from equation (32) through replacing  $U_{pq}(\hat{k}_s, \hat{k}_i)$  by  $U_{cc}(\hat{k}_s, \hat{k}_i)$  with:

$$U_{RR}(\hat{k}_s, \hat{k}_i) = \frac{1}{2} \left\{ U_{vv}(\hat{k}_s, \hat{k}_i) + U_{hh}(\hat{k}_s, \hat{k}_i) + j \left( U_{hv}(\hat{k}_s, \hat{k}_i) - U_{vh}(\hat{k}_s, \hat{k}_i) \right) \right\} \quad (\text{b.5})$$

$$U_{RL}(\hat{k}_s, \hat{k}_i) = \frac{1}{2} \left\{ U_{vv}(\hat{k}_s, \hat{k}_i) - U_{hh}(\hat{k}_s, \hat{k}_i) + j \left( U_{hv}(\hat{k}_s, \hat{k}_i) + U_{vh}(\hat{k}_s, \hat{k}_i) \right) \right\} \quad (\text{b.6})$$

$$U_{LR}(\hat{k}_s, \hat{k}_i) = \frac{1}{2} \left\{ U_{vv}(\hat{k}_s, \hat{k}_i) - U_{hh}(\hat{k}_s, \hat{k}_i) - j \left( U_{hv}(\hat{k}_s, \hat{k}_i) + U_{vh}(\hat{k}_s, \hat{k}_i) \right) \right\} \quad (\text{b.7})$$

$$U_{LL}(\hat{k}_s, \hat{k}_i) = \frac{1}{2} \left\{ U_{vv}(\hat{k}_s, \hat{k}_i) + U_{hh}(\hat{k}_s, \hat{k}_i) - j \left( U_{hv}(\hat{k}_s, \hat{k}_i) - U_{vh}(\hat{k}_s, \hat{k}_i) \right) \right\} \quad (\text{b.8})$$

The bistatic scattering coefficient  $\gamma_{PQ}^s(\hat{k}_s, \hat{k}_i)$  due to short capillary wave can be obtained from equation (72) through replacing  $G_{pq}(\hat{k}_s, \hat{k}_i)$  in equation (70) by  $G_{cc}(\hat{k}_s, \hat{k}_i)$  with:

$$G_{RR}(\hat{k}_s, \hat{k}_i) = \frac{1}{2} \left\{ G_{vv}(\hat{k}_s, \hat{k}_i) + G_{hh}(\hat{k}_s, \hat{k}_i) + j \left( G_{hv}(\hat{k}_s, \hat{k}_i) - G_{vh}(\hat{k}_s, \hat{k}_i) \right) \right\} \quad (\text{b.9})$$

$$G_{RL}(\hat{k}_s, \hat{k}_i) = \frac{1}{2} \left\{ G_{vv}(\hat{k}_s, \hat{k}_i) - G_{hh}(\hat{k}_s, \hat{k}_i) + j \left( G_{hv}(\hat{k}_s, \hat{k}_i) + G_{vh}(\hat{k}_s, \hat{k}_i) \right) \right\} \quad (\text{b.10})$$

$$G_{LR}(\hat{k}_s, \hat{k}_i) = \frac{1}{2} \left\{ G_{vv}(\hat{k}_s, \hat{k}_i) - G_{hh}(\hat{k}_s, \hat{k}_i) - j \left( G_{hv}(\hat{k}_s, \hat{k}_i) + G_{vh}(\hat{k}_s, \hat{k}_i) \right) \right\} \quad (\text{b.11})$$

$$G_{LL}(\hat{k}_s, \hat{k}_i) = \frac{1}{2} \left\{ G_{vv}(\hat{k}_s, \hat{k}_i) + G_{hh}(\hat{k}_s, \hat{k}_i) - j \left( G_{hv}(\hat{k}_s, \hat{k}_i) - G_{vh}(\hat{k}_s, \hat{k}_i) \right) \right\} \quad (\text{b.12})$$

## Attachment C to Annex

### Simple approximations

For incidence angles  $\theta_i$  and scattering angles  $\theta_s$  below 60 degrees, and for azimuth scattering angles  $\varphi_s$  within  $\pm 5$  degrees of the forward scattering plane ( $\varphi_s = \varphi_i = 0^\circ$ ), the cross polarized terms in equations (a.5) to (a.24) could be neglected leading to the simplifications reported below. In so doing, yields an error of less than 5%. Within the forward scattering plane ( $\varphi_s = \varphi_i = 0^\circ$ ), for the above incident and scattering angles, the error is negligible.

RHCP incident and vertical scattered power	$\gamma_{vR} = \frac{1}{2} \gamma_{vv}$
RHCP incident and horizontal scattered power	$\gamma_{hR} = \frac{1}{2} \gamma_{hh}$
LHCP incident and vertical scattered power	$\gamma_{vL} = \frac{1}{2} \gamma_{vv}$

LHCP incident and horizontal scattered power	$\gamma_{hL} = \frac{1}{2}\gamma_{hh}$
Vertical incident and RHCP scattered power	$\gamma_{Rv} = \frac{1}{2}\gamma_{vv}$
Horizontal incident and RHCP scattered power	$\gamma_{Rh} = \frac{1}{2}\gamma_{hh}$
Vertical incident and LHCP scattered power	$\gamma_{Lv} = \frac{1}{2}\gamma_{vv}$
Horizontal incident and LHCP scattered power	$\gamma_{Lh} = \frac{1}{2}\gamma_{hh}$

## Attachment D to Annex

### Sea surface height spectra model

The sea surface height spectrum is divided into two spectra: large-scale (gravity) spectrum and small-scale (capillary) spectrum, which are denoted by  $W_l(\kappa, \psi)$  and  $W_s(\kappa, \psi)$ , respectively. The large-scale spectrum is noted for reference but is not directly needed. The small-scale spectrum is related to the sea surface directional spectrum,  $W(\kappa, \psi)$ , as follows:

$$W_s(\kappa, \psi) = \begin{cases} 0 & \text{if } \kappa < \kappa_d \\ W(\kappa, \psi) & \text{otherwise} \end{cases} \quad (\text{d.1})$$

where  $\kappa_d$  is the two-scale cut-off height wavenumber, and  $(\kappa, \psi)$  are the polar coordinates of the height wavenumbers in the upwind and crosswind directions associated with the rectangular coordinates of the surface slopes ( $S_u, S_c$ ). The directional spectrum  $W(\kappa, \psi)$  is as follows:

$$W(\kappa, \psi) = \kappa^{-1} S(\kappa) \varphi(\kappa, \psi) \quad (\text{d.2})$$

where  $S(\kappa)$  is the isotropic (omni-directional) spectrum function, and  $\varphi(\kappa, \psi)$  is the angular spreading function. The isotropic spectrum,  $S(\kappa)$ , is given by:

$$S(\kappa) = \left( \frac{B_l + B_h}{\kappa^3} \right) G^\gamma \exp \left\{ -1.25 \left( \frac{\kappa_p}{\kappa} \right)^2 \right\} \quad (\text{d.3})$$

and  $B_l$  is the wave spectrum for long gravity waves:

$$B_l = 0.003 \Omega^{0.5} \frac{U_{10}}{\Omega C(\kappa)} \exp \left\{ \frac{-\Omega}{\sqrt{10}} (\sqrt{\kappa/\kappa_p} - 1) \right\} \quad (\text{d.4})$$

$$G = \begin{cases} 1.7 & \text{if } \Omega < 1 \\ 1.7 + 6.0 \log_e(\Omega) & \text{if } 1 \leq \Omega < 5 \\ 2.7 \Omega^{0.57} & \text{if } \Omega \geq 5 \end{cases} \quad (\text{d.5})$$

$$\gamma = \exp \left\{ -(\sqrt{\kappa/\kappa_p} - 1)^2 / 2 \xi^2 \right\} \quad (\text{d.6})$$

$$\xi = \begin{cases} 0.08(1 + 4\Omega^{-3}) & \text{if } \Omega < 5 \\ 0.16 & \text{if } \Omega \geq 5 \end{cases} \quad (\text{d.7})$$

$$C(\kappa) = \sqrt{g \{1 + (\kappa/\kappa_m)^2\}} / \kappa \quad (\text{d.8})$$

$$\kappa_p = g \left\{ \frac{\Omega}{U_{10}} \right\}^2, \quad g = 9.81, \quad \kappa_m = 364.52 \quad (\text{d.9})$$

$B_h$  is wave spectrum for short capillary waves:

$$B_h = 0.5\alpha_m \left( \frac{0.232}{C(\kappa)} \right) \exp \left\{ -0.25 \left( \frac{\kappa}{\kappa_m} - 1 \right)^2 \right\} \quad (\text{d.10})$$

$$\alpha_m = 0.014(u/0.232) \quad (\text{d.11})$$

$$u = U_{10} \sqrt{0.001(0.81 + 0.065U_{10})} \quad (\text{d.12})$$

and  $\Omega$  is the inverse wave age. The sea is considered to be:

- fully developed when  $\Omega$  has values close to 0.84,
- mature when  $\Omega$  has values close to 1, and
- young when  $\Omega$  has values  $> 2$ .

$U_{10}$  is the wind speed (typically between 3 m/s and 33 m/s) at a height of 10 m above the sea surface, and  $u$  is the friction velocity (i.e. the wind speed at the sea surface).  $\gamma$  in equation (d.3) is the water surface tension, and  $g$  in equation (d.5) is the water acceleration due to gravity in  $\text{m/s}^2$ .

The angular spreading function  $\varphi(\kappa, \psi)$  in equation (d.2) provides the azimuth dependence of the directional spectrum  $W(\kappa, \psi)$  given by:

$$\varphi(\kappa, \psi) = \frac{1}{2\pi} \{1 + \Delta(\kappa) \cos(2\psi)\} \quad (\text{d.13})$$

where  $\psi$  corresponds to the upwind direction, and  $\Delta(\kappa)$  is the angular dependence amplitude:

$$\Delta(\kappa) = \tanh \left\{ \frac{\log_e(2)}{4} + 4 \left( \frac{\Omega C(\kappa)}{U_{10}} \right)^{2.5} + \frac{0.13u}{0.232} \left( \frac{0.232}{C(\kappa)} \right)^{2.5} \right\} \quad (\text{d.14})$$

Note that  $C(\kappa)$  in equation (d.4) goes to  $\infty$  when  $\kappa$  goes to zero. However, when  $\kappa$  goes to zero,  $S(\kappa)$  also goes to zero. As a result, when  $\kappa = 0$ , set  $S(\kappa) = 0$  without further calculation.

## Attachment E to Annex

### Interference power of a reflected signal from the sea surface into a receiver

#### E.1 Introduction

The bistatic scattered power  $P_{rp}$  from the sea surface received by a receive antenna with linear polarization  $p$  is the sum of two components: a coherent component  $P_{cp}$ , and a diffuse (incoherent) component  $P_{dp}$ .

$$P_{rp} = P_{cp} + P_{dp} \quad (\text{e.1})$$

The following sections provide calculations of the received power for: a) the general case and b) approximations for the specific case of a transmitter in GEO orbit and a receiver in LEO orbit.

## E.2 Coherent received power

For identical transmit (incident) and receive (scattered) linear polarizations,  $p$ , the received coherent power,  $P_{cp}$  (W), is:

$$P_{cp} = \frac{P_{tp}G_{tp}L_{tp}}{4\pi(R_t+R_r)^2} \frac{\lambda^2 G_{rp}L_{rp}L_d}{4\pi} \gamma_{pp}^c \quad (\text{W}) \quad (\text{e.2})$$

where:

- $P_{tp}$  : transmitted power with polarization  $p$  (W)
- $G_{tp}$  : gain of the transmit antenna in the direction of the reflection point on the surface of the Earth (linear)
- $R_t$  : range between the transmitter and the specular reflection point on the surface of the Earth (m)
- $R_r$  : range between the specular reflection point on the surface of the Earth and the receiving antenna (m)
- $G_{rp}$  : gain of the receive antenna in the direction of the specular reflection point on the surface of the Earth (linear)
- $L_{tp}$  : atmospheric loss (e.g. the gaseous attenuation) along the path from the interferer to the specular reflection point. The gaseous attenuation,  $A_{gas}$  (dB), can be calculated using Annex 1 or Annex 2 of Recommendation ITU-R P.676-12, in which case  $L_{tp} = 10^{-A_{gas}/10}$
- $L_{rp}$  : atmospheric loss (e.g. the gaseous attenuation) along the path from the specular reflection point to the receiving antenna. The gaseous attenuation,  $A_{gas}$  (dB), can be calculated using Annex 1 or Annex 2 of Recommendation ITU-R P.676-12, in which case  $L_{rp} = 10^{-A_{gas}/10}$
- $\lambda$  : wavelength (m)
- $L_d$  : divergence loss due to the Earth's curvature, given by:

$$L_d = \frac{1}{\left[ \left(1 + \frac{2R_e}{a \cos \theta}\right) \left(1 + \frac{2R_e \cos \theta}{a}\right) \right]} \quad (\text{e.3})$$

where:

- $a$  : average radius of the Earth (6 371 000 m)
- $R_e$  : effective range  $R_e = \frac{R_t R_r}{R_t + R_r}$  (m)
- $\theta$  : incident zenith angle.

### E.2.1 Transmitter in GEO orbit and a receiver in LEO orbit: coherent component

For the specular reflected component,  $R_t + R_r$  is the total range and  $4\pi(R_t + R_r)^2$  is the spreading loss.  $P_{tp}G_{tp}$  is the equivalent isotropically radiated power (e.i.r.p.). For a transmitter in GEO orbit and a receiver in low earth orbit (LEO), the approximation that  $R_t + R_r \cong R_t$  introduces a few percent error in the coherent term. In this case, equation (e.2) becomes:

$$P_{cp} = \frac{P_{tp}G_{tp}L_{tp}}{(4\pi R_t)^2} \lambda^2 G_{rp}L_{rp}L_d \gamma_{pp}^c \quad (\text{W}) \quad (\text{e.4})$$

$\gamma_{pp}^c$  is the coherent bistatic scattering coefficient given by equation (11) for linearly polarized incident and linearly polarized scattered waves. The corresponding polarization transformations in Attachments A, B and C can be used for other incident and scattered polarization pairs.

### E.3 Diffuse received power

The received diffuse power,  $P_{dp}$  (W), can be calculated using the conventional bistatic radar equation (e.g. equation (73) of Recommendation ITU-R P.452-16). The diffuse scattered power received by an antenna with polarization  $p$  due and transmit polarization  $q$  is:

$$P_{dp} = P_{tq} \frac{\lambda^2}{(4\pi)^3} \iint \frac{G_{rp}(\hat{k}_i)G_{tq}(\hat{k}_s)}{r_t^2 r_r^2} L_{tq}(\hat{k}_i) \gamma_{pq}^{dif}(\hat{k}_s, \hat{k}_i) \cos \theta_s L_{rp}(\hat{k}_s) dA \quad (\text{W}) \quad (\text{e.5})$$

where:

- $P_{tq}$  : transmit power with polarization  $q$  (W)
- $\hat{k}_i$  : incident direction at the scattering differential area
- $\hat{k}_s$  : scattered direction at the scattering differential area
- $G_{rp}(\hat{k}_i)$  : gain of the transmit antenna in the incident direction  $\hat{k}_i$  (linear)
- $G_{tq}(\hat{k}_s)$  : gain of the receive antenna in the receive direction  $\hat{k}_s$  (linear)
- $dA$  : differential scattering area within the surface ( $\text{m}^2$ )
- $r_t$  : range between the transmitter and the scattering differential area on the surface of the Earth (m)
- $r_r$  : range between the scattering differential area on the surface of the Earth and the receiver (m).

#### E.3.1 Transmitter in GEO orbit and a receiver in LEO orbit: diffuse component

The following approximation assumes the gain of the transmit antenna is constant over the receive antenna footprint (a reasonable assumption for a GEO transmitter with a moderate gain antenna and a LEO receiver with a high gain antenna), and the distances from the transmit antenna to the surface of the Earth and from the surface of the Earth to the receive antenna do not vary significantly over the receive antenna footprint. Then, equation (e.5) can be approximated by:

$$P_{dp} \cong \frac{P_{tq} G_{tq} \lambda^2 L_{tq}(\hat{k}_i) L_{rp}(\hat{k}_s)}{(4\pi R_t)^2} \gamma_{pq}^{dif}(\hat{k}_{s0}, \hat{k}_{i0}) \quad (\text{e.6})$$

where:

- $\hat{k}_{i0}$  : incident direction at the scattering differential area along the transmitting antenna main beam
- $\hat{k}_{s0}$  : scattered direction at the scattering differential area along the receive antenna main beam
- $R_t$  : range between the transmitter and the centre of the footprint, on the surface of the Earth, illuminated by the transmit antenna (m).

The polarization transformations in Attachments A, B and C can be used to calculate  $\gamma_{pq}^{dif}(\vec{r}_{t0}, \vec{r}_{r0})$  for incident and scattered polarizations other than linear-linear or circular-circular.